

A computational study on cannabinoid receptors and potent bioactive cannabinoid ligands: homology modeling, docking, de novo drug design and molecular dynamics analysis

Serdar Durdagi · Manthos G. Papadopoulos ·
Panagiotis G. Zoumpoulakis · Catherine Koukoulitsa ·
Thomas Mavromoustakos

Received: 3 March 2009 / Accepted: 17 May 2009 / Published online: 18 June 2009
© Springer Science+Business Media B.V. 2009

Abstract When X-ray structure of a ligand-bound receptor is not available, homology models of the protein of interest can be used to obtain the ligand-binding cavities. The stereo-electronic properties of these cavities are directly related to the performed molecular model coordinates. Thus, the use of different template structures for homology may result in variation of ligand-binding modes. We have recently reported the MD simulations of a potent CB ligand at bovine rhodopsin-based CB1 and CB2 receptors (Durdagi et al., *Bioorg Med Chem* 16:7377–7387, 2008). In this present study, a homology modeling study based on the β 2-adrenergic receptor for both CB1 and CB2 receptors was performed, and the results were compared with rhodopsin-based models. In addition, the role of membrane bilayers to the adopted conformations of potent AMG3 CB ligand has been analyzed for receptor-free and membrane-associated receptor systems. The performed MD trajectory analysis results have shown that *gauche* conformations at the terminal segment of the

alkyl side chain of AMG3 are not favored in solution. Different adopting dihedral angles defined between aromatic and dithiolane rings at the active sites of the CB1 and CB2 receptors, which are adapted lead to different alkyl side chain orientations and thus, may give clues to the medicinal chemists to synthesize more selective CB ligands. The binding sites of receptors derived by rhodopsin-based models have been regenerated using the β 2-adrenergic based template receptors. The re-obtained models confirmed the ligand-binding pockets that were derived based on rhodopsin.

Keywords Cannabinoids · AMG3 ·
Conformational analysis · 3D QSAR ·
Homology modeling · CB1 and CB2 receptors

Abbreviations

CB	Cannabinoid
CB1	First cannabinoid receptor
CB2	Second cannabinoid receptor
MD	Molecular dynamics
Δ^8 -THC	Δ^8 -Tetrahydrocannabinol
AMG3	(-)-2-(6a,7,10,10a-Tetrahydro-6,6,9-trimethylhydroxy-6H-dibenzo[b,d]pyranyl)-2-hexyl-1,3dithiolane

Electronic supplementary material The online version of this article (doi:10.1007/s11030-009-9166-4) contains supplementary material, which is available to authorized users.

S. Durdagi (✉) · M. G. Papadopoulos · P. G. Zoumpoulakis ·
C. Koukoulitsa · T. Mavromoustakos (✉)
Institute of Organic and Pharmaceutical Chemistry, The National
Hellenic Research Foundation, 48 Vas. Constantinou Avenue,
11635 Athens, Greece
e-mail: durdagis@eie.gr; durdagis@yahoo.de

S. Durdagi
Department of Biology, Chemistry, and Pharmacy, Freie
Universität Berlin, Takustr. 3, 14195 Berlin, Germany

T. Mavromoustakos
Department of Chemistry, University of Athens,
15784 Athens, Greece
e-mail: tmavro@eie.gr

Introduction

One of the frequently faced problems in drug design is to discover the bioactive conformation of a molecule defined as the proper and unique conformation that fits with its target-binding site and triggers a biological response. The relationship between the conformations of bioactive molecules with their pharmacological profiles has been well established [1, 2]. However, as it appears in the literature, for the same

biologically interesting molecule more than one conformation is proposed as putative bioactive [3–10]. Selection and knowledge of the low energy conformations of a ligand at the binding site of a receptor assist in the rational approach to drug design [11]. On the other hand, the bioactive conformation of a drug compound is not necessarily identical to the lowest energy conformation in solution [1, 2]. This is attributed to the fact that drug molecules may contain flexible segments that can easily adopt conformations with higher energies in the biological matrices or at the active site of the receptor due to different favorable interactions which compensate the increase of energy. Nonetheless, a very high energy conformation that is excluded from the population of conformations in solution cannot be biologically active [1, 12]. Predicting flexible chain conformations of a ligand at the biological matrices and, particularly at the binding site of the receptor, is a complex issue for rational drug design because a flexible chain can adopt various conformations, depending on the biological environment which it interacts. In addition, in three dimensional quantitative structure–activity relationships (3D QSAR) studies, the selection of bioactive conformations of compounds being studied and their alignments are the two most important steps. These steps not only affect the output of the analysis, but they also contribute to the design of novel molecules [13]. If the X-ray structure of a target protein and the experimental data concerning the ligand–receptor complex are available, the selection of the bioactive conformer is a simpler procedure, and the molecules can be aligned with greater credibility. When no experimental structural information is available, molecular modeling techniques can be used to analyze the bioactive conformations of the ligand and the biological target [13].

Until now, C-1'-dithiolane Δ^8 -tetrahydrocannabinol (Δ^8 -THC) analog (-)-2-(6a,7,10,10a-tetrahydro-6,6,9-trimethylhydroxy-6H-dibenzo[b,d]pyranyl)-2-hexyl-1,3 dithiolane (AMG3) (Fig. 1i) is considered as one of the most potent synthetic cannabinoid (CB) ligands (K_i for CB1 and CB2 receptors are 0.32 and 0.52 nM, respectively) [14]. Structure–activity relationships (SAR) and 3D QSAR studies on classical CBs have demonstrated that the alkyl side chain is the most critical structural segment for the receptor activation [14–18]. Reported low energy conformations of Δ^8 -THC analogs using NMR spectroscopy and molecular modeling studies in solution or in lipid bilayer derived different low energy conformations [6–10]. The derived conformations differ in the alkyl side chains (i.e., conformers **a** and **b**) or in the ABC tricyclic segments (i.e., conformers **a** and **aa** in Fig. 1i). For example, in both conformers **a** and **aa**, proposed for Δ^8 -THC analogs, and shown in the Fig. 1i, the alkyl chain adopts an orthogonal orientation relative to the horizontal plane of ring A; however, B and C rings have different geometries (i.e., ring B has half chair-like and boat-like forms, in conformers **a** and **aa**, respectively). In conformer

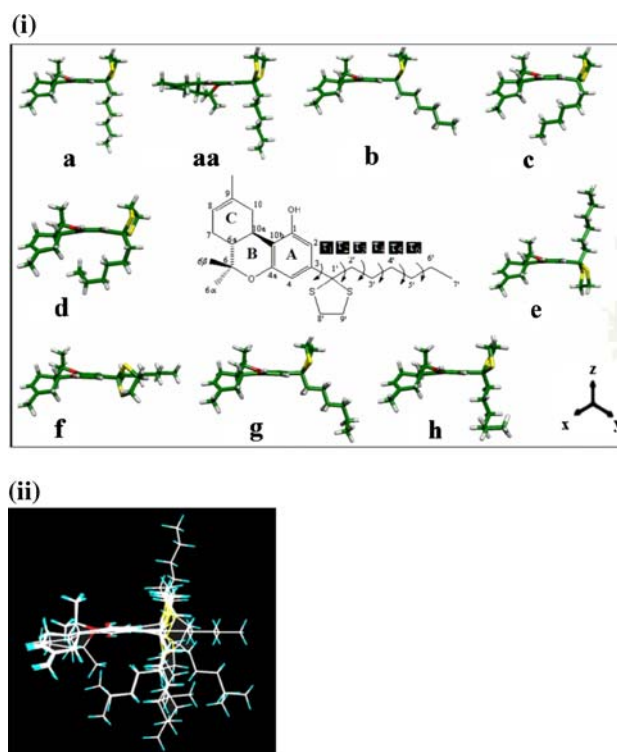


Fig. 1 (i) Molecular structure of AMG3 and its low energy conformers. Conformers **a**, **aa**, **b**, and **c** have been proposed from reported [6–10] low energy conformers of Δ^8 -THC analogues and conformers **a–h** except conformer **aa** are derived performing MC analysis. Dihedral angles of the alkyl side chain are assigned on the central structure (τ_1 , C2–C3–C1'–C2'; τ_2 , C3–C1'–C2'–C3'; τ_3 , C1'–C2'–C3'–C4'; τ_4 , C2'–C3'–C4'–C5'; τ_5 , C3'–C4'–C5'–C6'; τ_6 , C4'–C5'–C6'–C7'). (ii) Superimposition of the conformers shown in (i) of AMG3

b, the alkyl chain has been extended away from the ABC tricyclic segment while in conformer **c**, the alkyl chain has been wrapped toward the tricyclic part (Fig. 1i).

Conformational studies of AMG3 using a combination of 1D and 2D NMR spectroscopy as well as molecular modeling techniques showed that the alkyl side chain adopts a perpendicular orientation relative to the horizontal plane of ring A of AMG3 [6]. The conformation of the flexible 1',1' dimethylheptyl side chain was also analyzed using a combination of theoretical studies and NMR experiments for classical CB (-)-9-nor-9 β -hydroxy(dimethylheptyl)-hexahydrocannabinol and nonclassical CBs CP47,497, CP55, 244 and CP55, 940 by Xie et al. [19–21]. Results showed that the alkyl side chain is almost perpendicular to the horizontal plane of the ring A.

CBs are predicted to exert their biological action in the trans-membrane (TM3–TM7) helices of G-protein-coupled receptors (GPCR) [22, 23]. Reported experimental results suggest that analgesic activity of CBs can be related with two sequential criteria: (i) “proper” topology and orientation of the drug in the membrane bilayer; (ii) diffusion and “appropriate” fit of the drug in the receptor [24]. CBs are lipophilic molecules and are considered to first interact with the

lipid microenvironment that surrounds the membrane-associated protein and then diffuse laterally at the active site of the receptor [25]. Therefore, it is important to understand the conformational properties of a drug molecule into the lipid microenvironment. Membranes do not lend themselves in a detailed analysis of their structural and dynamical properties by means of a single physicochemical method because of their complexity and instability [24]. Thus, it is preferable to combine several experimental and/or computational methods seeking to obtain molecular information on the interactions of drugs with membranes [24]. Biophysical studies using different techniques [e.g., solid-state NMR spectroscopy, X-ray diffraction, Raman spectroscopy, infrared (IR) spectroscopy, differential scanning calorimetry (DSC), etc.] in combination with molecular modeling studies assist in the determination of drug–membrane interactions and the role of membrane in the putative bioactive conformation of the drug molecule. The results of recent 3D QSAR studies using theoretical calculations and molecular docking simulations support the above statement [18].

The effect of the cannabinomimetic drug AMG3 on the thermotropic and structural properties of dipalmitoyl-*sn*-glycero-3-phosphorylcholine (DPPC) liposomes have been studied by X-ray diffraction and DSC methodologies by Mavromoustakos et al. [26]. AMG3 was found to efficiently fluidize domains of the lipids in the L'_β gel phase and to perturb the regular multibilayer lattice. In the liquid crystalline L_α phase, AMG3 was also found to cause irregularities in packing, suggesting that the drug induces local curvature. Biophysical studies by Makriyannis et al. [24] have also provided detailed information for the topography, the stereochemistry, and the dynamic properties of the CB ligand–membrane interactions by applying neutron diffraction, solid-state ^2H -NMR, DSC, and small angle X-ray spectroscopy of Δ^8 -THC [27–34]. In these studies, THC assumes an “awkward” orientation in the bilayer with the long axis of its tricyclic system being perpendicular to the bilayer chains, while its aliphatic side chain orients parallel to the chains of the membrane phospholipids [24].

The existing experimental evidence recorded by our group, combined with theoretical calculations as well as 3D QSAR studies [17], show that the alkyl side chain of AMG3 adopts an orthogonal geometry relative to the horizontal plane of the ring A of the rigid tricyclic segment in solution. In the past, we had applied a conformational analysis study of AMG3 using molecular dynamics (MD) simulations in solution and at the active sites of bovine rhodopsin-based homology models of the CB1 and CB2 receptors [35]. The MD trajectory analysis results showed that the ligand can adopt both *cis* and *trans* conformations at the active site of the CB1 receptor for τ_3 – τ_6 dihedral angles in the alkyl chain; however, in CB2 receptor, conformers prefer to adopt only *trans* conformation [35]. In addition, low energy conformers of AMG3

at the active site of the CB1 receptor adopt a *cis* conformation for the τ_1 but a *trans* conformation at the binding site of the CB2 receptor [35]. This leads to different orientations of classical CBs at the active site of the receptors, and results can be used for the design of selective CB ligands [35]. In this research activity, we expand our previous study [35]. Clearly, the stereoelectronic properties of a binding cavity are related to the used molecular model coordinates. The use of different template structures for homology modeling may cause variations in the ligand-binding modes. A recent comparative study between bovine rhodopsin and human β_2 adrenergic-based homology models by Yuzlenko et al. [36] revealed several differences in ligand-binding pockets. Therefore, in this study work, homology models of the CB1 and the CB2 receptors were attempted, based on human β_2 -adrenergic receptor (PDB code: 3D4S) [37] and binding pockets have been compared with the bovine rhodopsin-based CB models. In addition, we examined the effects of membrane bilayers to the adopted conformations of potent CB analog AMG3 using both free receptor and membrane-associated receptor systems and based on derived information several predicted high affinity analogs of AMG3 for CB1 and CB2 receptors were proposed using de novo drug design studies. Our stepwise study strategy used is based on: (i) Monte Carlo (MC) conformation analysis and clustering of the resulted conformers; (ii) comparative molecular mechanics and quantum mechanics (MM/QM) geometry optimization calculations of conformers; (iii) rotational energy barrier calculations employing semi-empirical calculations; (iv) testing the stability of conformations of ligand with MD simulations at solvent and at the membrane bilayer environments; (v) docking of the stable potent putative bioactive conformations of ligand at the shared rhodopsin-based homology models of the CB receptors; (vi) MD simulations of docked complexes at solvent and at membrane bilayer environments; (vii) homology modeling studies of CB1 and CB2 receptors based on β_2 -adrenergic receptor; (viii) clustering the produced CB1 and CB2 receptor models and selection of the best models; (ix) comparison of obtained results based on the two used different receptor models. For clarity, the results of this study has been summarized in a scheme (see Fig. 2). Since in this study we expand on our previously published study [35], some parts of above steps (i, ii, iv, and v) are common and, therefore, these steps will not be covered in great detail in this article.

Methods

MC simulation

MC simulation was performed using QUANTA/CHARMm software [38] to investigate a complete conformational space

tolerance was set to $1000 \text{ kJ}(\text{mol nm})^{-1}$). The system was then equilibrated via 250 ps simulation with a time step of 2 fs; subsequently, a 2.5 ns simulation was performed at 300 K and 1 bar with a time step of 2 fs using Berendsen thermostat [45] and Parrinello-Rahman barostat [53] algorithms. All the bonds were constrained using the LINCS algorithm [47]. (iii) *Membrane-associated receptor MD simulations*: The lipid used “in solution” calculations was employed here; however, the lipid extended by $4 \times 4 \times 1$ in xyz to have enough area of lipid for the protein merging. Same running parameters within solution (DPPC molecules) were used. (iv) *MD simulations at the homology modeling step of the receptors*: The MD simulations were performed with GROMACS 3.3.1 software package [44] using gmX force field [45]. Same parameters as in (i) were used except equilibration time which was set as 100 ps with a time step of 2.0 fs. The orientation of receptor regarding to the lipid membrane was corrected based on the reported literature [54, 55, 67]. In order to examine convergence criteria, potential energy versus time plots have been employed in the Supporting Material (Fig. S7).

Molecular docking studies

Flexible docking studies have been performed using FlexX program of Sybyl molecular modeling package [57]. The physicochemical model behind FlexX can be divided into three parts: the analysis of the conformational space of the ligand, the model of protein–ligand interactions, and the scoring function. The scoring function of FlexX, developed by Böhm [56] to rank the solutions, is an estimation of the free binding energy ΔG of the protein–ligand complex:

$$\begin{aligned} \Delta G_{\text{binding}} = & \Delta G_{\text{O}} + \Delta G_{\text{rot}} \times N_{\text{rot}} + \Delta G_{\text{hb}} \sum_{\text{H-bonds}} f(\Delta R, \Delta \alpha) \\ & + \Delta G_{\text{ion}} \sum_{\text{ionic_int}} f(\Delta R, \Delta \alpha) \\ & + \Delta G_{\text{arom}} \sum_{\text{aromatic}} f(\Delta R, \Delta \alpha) \\ & + \Delta G_{\text{lipo}} \sum_{\text{lipo_cont.}} |A_{\text{lipo}}| \end{aligned}$$

$$f(\Delta R, \Delta \alpha) = f1(\Delta R)f2(\Delta \alpha)$$

$$f1(\Delta R) = \begin{cases} 1 & \Delta R \leq 0.2 \text{ \AA} \\ 1 - (\Delta R - 0.2)/0.4 & \Delta R \leq 0.6 \text{ \AA} \\ 0 & \Delta R > 0.6 \text{ \AA} \end{cases}$$

$$f2(\Delta \alpha) = \begin{cases} 1 & \Delta \alpha \leq 30^\circ \\ 1 - (\Delta \alpha - 30)/50 & \Delta \alpha \leq 80^\circ \\ 0 & \Delta \alpha > 80^\circ \end{cases}$$

where, $f(\Delta R, \Delta \alpha)$ is a scaling function that penalizes deviations from ideal geometry. ΔG_{O} is a contribution to the binding energy that does not directly depend on any specific interaction with the protein [56]. It may be rationalized as a reduction of binding energy due to overall loss of translational and rotational entropy of ligand. ΔG_{rot} describes the loss of binding energy due to freezing of internal degrees of freedom in the ligand. N_{rot} is the number of rotatable bonds that are immobilized in the complex. ΔG_{hb} represents the contribution from an ideal hydrogen bond. ΔG_{ion} describes the contribution from an unperturbed ionic interaction. ΔG_{arom} accounts for the interactions of aromatic groups and ΔG_{lipo} represents the contribution from lipophilic interactions. It is assumed that such interactions are proportional to A_{lipo} , the lipophilic contact surface between the protein and the ligand [56].

The 3D models of the CB1 and CB2 receptors based on rhodopsin from Tuccinardi et al. [66] have been used for the initial docking experiments; however, the critical binding site residues were determined considering all the 3D models of CB receptors of Salo et al. [64], Shim et al. [65], and Tuccinardi et al. [66]. Docking results have been rechecked by using our homology modeling studies based on $\beta 2$ adrenergic receptor (PDB code: 3D4S).

Homology modeling

The Biopolymer module of Sybyl has been used for the sequence alignment studies. The initial structure was taken from the cholesterol bound form of human $\beta 2$ adrenergic receptor (PDB code: 3D4S). The water molecules and the cholesterol were removed from the system and seven TM receptors were picked up from the pdb file. The sequence alignment was performed with Sybyl Biopolymer module and initial geometry optimization calculations have been carried out with Powel algorithm using Tripos force field. Subsequently, these receptors have been subjected to 1ns MD simulations. Before the simulations, geometry optimization of receptors have been performed without constrains using steepest descent integrator for 10000 steps with the minimization tolerance of $100 \text{ kJ}(\text{mol nm})^{-1}$. Cluster analysis of obtained coordinate file of trajectories has been performed with g_cluster module of Gromacs with Gromos option. RMSD comparison of obtained representative model conformers of clusters with rhodopsin-based models has been performed with Accelrys DS 2.0 program.

De novo drug design

LeapFrog algorithm under Sybyl was used to automatically generate a series of ligands for the binding pocket of a receptor. Leapfrog is a second generation de novo drug discovery program for the design of potentially active compounds,

using molecular evolution or electronic screening, by repeatedly making structural changes and then either keeping or discarding the obtained results, depending on the binding energy results. There are two starting input options to generate site point probe atoms that will be used in the binding energy calculations. These are the pharmacophore model or a receptor structure. The charge of the site point probe atom is positive, negative, or lipophilic, and its value is compared with ± 1.0 . If the value is smaller than $+1.0$, it is lipophilic, if the value is bigger than $+1.0$, site points seek a negative atom, and if the value is less than -1.0 , site points seek a positive atom in the fragment. Binding energy calculations in LeapFrog were performed by steric, electrosteric, and hydrogen-bonding enthalpies of ligand cavity binding using the Tripos force field under Sybyl molecular modeling package (v. 6.8). As with many de novo drug design programs, central operation of LeapFrog is the processing loop. In each pass through the loop, a type of move is selected randomly. If the move succeeds, a new structure is evaluated. A new ligand which passes evaluation is added to the pool of ligands available for the next move. The fragments used in JOIN, FUSE, and BRIDGE are stored as a molecular data base in Sybyl. A hydrogen atom is chosen within the selected ligand, randomly; and a local energy check is performed on its cavity environment within a 3.0 \AA radius. If steric interactions are not favorable over more than half of the environment volume, the hydrogen atom is sterically excluded. If the first chosen hydrogen is not accessible, another one is chosen, randomly until an accessible one is found. If no accessible hydrogens are found, the JOIN move fails. The FUSE move process is similar to that of JOIN: environment checks for

steric accessibility are performed as in JOIN move; however, in a FUSE attempt, existence of a ring bond flanked by hydrogen in both ligand and fragment are required. Thus, FUSE move aims to fuse (usually rings) starting ligand and fragment from data base. The BRIDGE move attempts to bridge available fragments.

As an initial basic procedure of LeapFrog, site-point probe atoms were generated using the receptor cavity as well as a pharmacophore model inferred from the PLS results options. Template compound AMG3 was selected as starting structure. First, the OPTIMIZE module was used for the improvement in binding energy. Second, several moves such as JOIN, FUSE, BRIDGE and OPTIMIZE options were used after the initial run of 100 moves taking into account the synthetic difficulties. The derived ligands that had the best binding energy were used for repeating the cycle of 5,000 moves.

Results and discussion

Selection of low energy conformers of AMG3

Low energy conformers of AMG3 are produced using MC conformational search analysis which derived 1,000 conformers [35]. These conformers were clustered into eight different groups based on the dihedral angle criterion [35]. The lowest energy conformers from each cluster have been selected for further analysis. The number of conformers for each of the eight clusters has been shown in the Table 1. Cluster analysis showed that conformers **a** (perpendicular

Table 1 Number of conformers in each obtained cluster by MC analysis and comparison of the total energies of conformers of AMG3 using MM and QM methods

Conformer	Number of conformers in each obtained cluster by MC analysis	MM relative energy (kcal mol ⁻¹)					QM geometry optimization (B3LYP/6-31G*), total energy (kcal mol ⁻¹)
		Torsional energy	VDW energy	Electrostat. energy	Other contributions ^a to MM energy	Total energy	
a	188	5.520	-3.821	-5.820	6.621	2.499	-1205537.64
aa	-	9.147	-2.674	-5.936	8.211	8.748	-1205537.64
b	147	5.550	-3.055	-5.817	6.688	3.366	-1205536.39
c	42	6.412	-5.857	-5.696	7.647	2.508	-1205535.09
d	102	6.493	-6.877	-5.676	8.157	2.097	-1205537.65
e	156	5.528	-3.877	-5.782	6.558	2.427	-1205537.65
f	92	6.180	-2.894	-5.693	6.773	4.366	-1205536.08
g	134	5.699	-3.013	-5.788	7.120	4.018	-1205535.62
h	139	5.783	-4.094	-5.726	7.507	3.470	-1205536.17
Average ^b	111	6.257	-4.018	-5.770	7.254	3.723	-1205536.38

^a Other contributions: bond stretching energy, angle bending energy, out of plane bending energy.

^b Average results do not include conformer **aa** for QM total energies, because conformer **aa** is transformed to conformer **a** when QM geometry optimization is applied

orientation of alkyl chain relative to the rigid ring segment) and wrapped conformer **c** (wrapped conformations are defined as those conformations adopting *gauche* τ_3 – τ_4 dihedral angles at the alkyl chain) have the highest and the smallest group member population, respectively. Among the eight lowest energy conformers, three conformers (**a**, **b**, and **c** of AMG3 in Fig. 1i) are identical with those reported conformations of Δ^8 -THC analogs [6, 8–10] using experimental results and/or molecular modeling techniques, while other five conformations (conformers **d**–**h** of AMG3 in Fig. 1i) differed. Conformer **aa** was not obtained by MC cluster analysis. Figure 1ii shows superimposition of conformers of AMG3 shown in Fig. 1i.

Geometry optimization calculations

The MM geometry optimization has been applied using SYBYL molecular modeling package [57]. According to MM calculations, conformer **aa** has significantly high total energy (~ 8.8 kcal mol $^{-1}$) due to its high torsional energy, while other conformers have a similar energy plateau within the range of ~ 2.3 kcal mol $^{-1}$ (Table 1). The high energy conformer **aa** of AMG3 has been transformed to conformer **a** at the ab initio B3LYP/6-31G* [58, 59] level optimizations. QM calculations show that all the low energy conformers are almost isoenergetic (maximum total energy difference between the conformers is ~ 2.5 kcal mol $^{-1}$, Table 1). In order to examine the solvent effect over geometrical properties of conformers, the vacuum medium has been modified to amphiphilic environment. The dielectric constant ϵ was set to 45, simulate DMSO, because it provides an amphiphilic environment, which mimics physiological conditions, and therefore, it is appropriate for investigating biological structures [60]. It is observed that the effect of DMSO continuum model to the analyzed conformers compared to gas phase is very limited as it is depicted by the small RMSD value between the conformers in gas phase and in DMSO continuum model (Table 2). Dihedral angles of the alkyl side chain segment of all conformers applying full geometry optimization with MM and QM methods in gas phase and in DMSO continuum model are presented in Table 2.

Rotational energy barrier calculations

In order to characterize the conformational flexibility properties of AMG3, rotational energy barriers were estimated using torsional grid scan analysis with semi-empirical method PM3 [61]. Six rotatable torsional angles of AMG3, shown in Fig. 1i and defined in its figure legend, were analyzed (Fig. 3). The analysis is initiated with τ_1 and the energetically lowest structure (optimal dihedral angle) is used for the next torsional angle analysis. Rotation around dihedral angles τ_4 – τ_6 showed similar energy profiles and rotational

Table 2 Values of dihedral angles corresponding to the alkyl chain part for low energy conformers of AMG3 derived by applying full geometry optimization with MM (left) and QM (right) with B3LYP/6-31G* level of theory

Conformer	τ_1 (degree)		τ_2 (degree)		τ_3 (degree)		τ_4 (degree)		τ_5 (degree)		τ_6 (degree)		RMSD														
	MM	QM	MM	QM	MM	QM	MM	QM	MM	QM	MM	QM	MM	QM													
	$\epsilon = 1$	$\epsilon = 45$	$\epsilon = 1$	$\epsilon = 45$	$\epsilon = 1$	$\epsilon = 45$	$\epsilon = 1$	$\epsilon = 45$	$\epsilon = 1$	$\epsilon = 45$	$\epsilon = 1$	$\epsilon = 45$	$\epsilon = 1$	$\epsilon = 45$													
a	73.8	73.2	63.3	65.3	57.8	57.8	61.1	61.3	178.9	179.0	181.1	181.7	179.7	180.5	180.2	180.0	180.0	180.2	180.8	180.0	180.0	180.1	180.0	0.25	0.75		
aa	78.1	78.1	63.3	65.3	56.7	56.8	61.1	61.3	178.5	178.5	181.1	181.7	179.3	180.5	180.2	180.1	180.1	180.2	180.8	180.2	180.8	180.0	180.0	180.1	180.0	0.01	0.75
b	82.0	82.0	81.5	77.2	181.0	181.0	184.0	176.5	179.8	179.8	185.3	182.2	180.0	180.0	180.6	180.0	180.0	180.0	180.5	179.6	180.0	180.0	179.9	180.0	0.00	3.86	
c	55.4	54.8	62.6	63.1	65.0	65.2	65.5	65.3	293.9	294.3	279.2	278.9	191.4	191.3	185.0	185.0	181.9	181.8	179.4	179.4	180.3	180.2	179.4	179.5	0.13	0.25	
d	55.7	55.2	61.4	59.0	68.9	69.1	66.7	68.6	300.8	301.2	281.5	285.5	191.0	190.9	186.8	186.2	176.5	176.4	176.5	177.7	63.9	63.7	65.9	66.0	0.12	2.08	
e	258.0	257.6	250.5	244.1	57.9	58.0	60.9	60.8	178.6	178.6	180.8	180.7	179.7	180.1	180.2	180.0	180.0	180.0	180.1	180.0	180.0	180.0	180.0	180.0	0.17	2.61	
f	187.4	187.0	187.2	187.1	176.9	177.0	175.6	175.6	176.6	176.5	177.8	177.8	179.5	179.5	179.6	179.9	179.9	179.9	179.5	179.5	180.0	180.0	180.1	180.1	0.17	0.06	
g	81.9	82.2	86.9	83.0	181.1	181.1	182.7	184.1	179.9	179.9	184.8	185.5	180.5	180.6	180.7	181.0	185.7	185.7	183.2	183.5	296.3	296.4	294.3	294.4	0.14	1.71	
h	103.1	103.7	116.1	128.3	302.9	302.9	298.0	297.3	182.6	182.6	178.9	178.0	186.5	186.6	184.2	181.8	302.0	302.1	296.6	295.4	302.3	302.3	297.2	297.3	0.25	5.11	

After optimization with QM, conformer **aa** is transformed to conformer **a**, therefore they have identical dihedral angles for the corresponding method

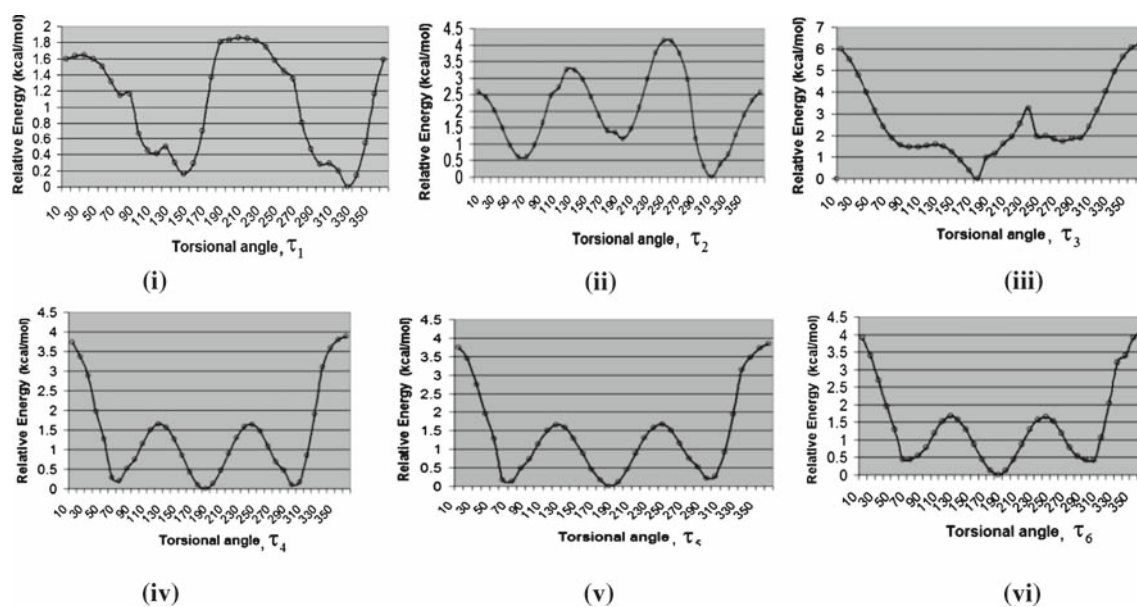


Fig. 3 Rotational energy barriers of AMG3 after applying grid scan analysis with consecutive optimization of dihedral angles (i) τ_1 , (ii) τ_2 , (iii) τ_3 , (iv) τ_4 , (v) τ_5 , and (vi) τ_6 . In the figure, relative energies

(differences of initial and final values of total energies with rotation) have been used instead of total energies for clarity

energy barriers are found to be $\sim 4 \text{ kcal mol}^{-1}$. The optimal dihedral angle was found to be $\sim 180^\circ$ and the local minima were observed at $\sim 60^\circ$ and $\sim 300^\circ$. Rotation around dihedral angles τ_1 and τ_2 showed a rather more complex energy profiles due to the presence of the tricyclic rigid ring system. Rotation around dihedral angle τ_3 showed the largest rotational energy barrier ($\sim 6 \text{ kcal mol}^{-1}$) and optimal dihedral angle value was found to be $\sim 180^\circ$ (Fig. 3).

MD simulations of conformers in solution

Computer simulations in general, and MD simulations in particular, are of increasing importance in revealing details of molecular motions as well as structural and microscopic properties of the solution, which are difficult to measure experimentally [62]. Heating increases the kinetic energy of the system which after equilibration at the given temperature overcomes any energy barriers close to the initial energy minimum. In order to examine the environmental effects over the structures, MD simulations were performed for all the examined conformers with the GROMACS 3.3.1 software package [44, 63] in two different environments (i) DMSO solvent and (ii) membrane bilayer. MD simulations were used to (i) further study the conformational space of AMG3 and (ii) explore the possibility of interconversion between conformers in amphiphilic environments.

- (i) *MD in DMSO*: Trajectory analysis results for the screening torsional angles of alkyl side chain of AMG3 throughout the simulations were reported previously by

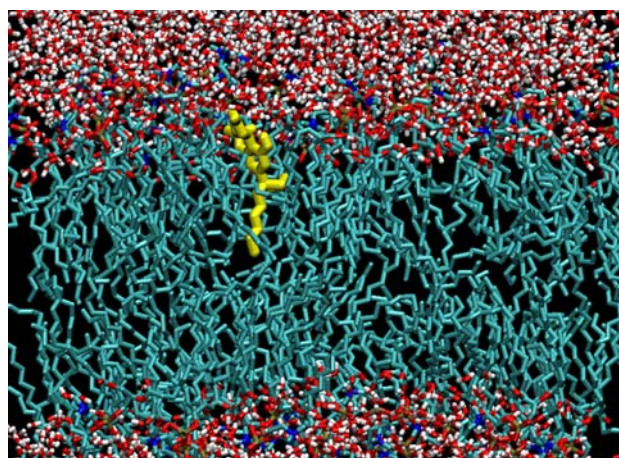
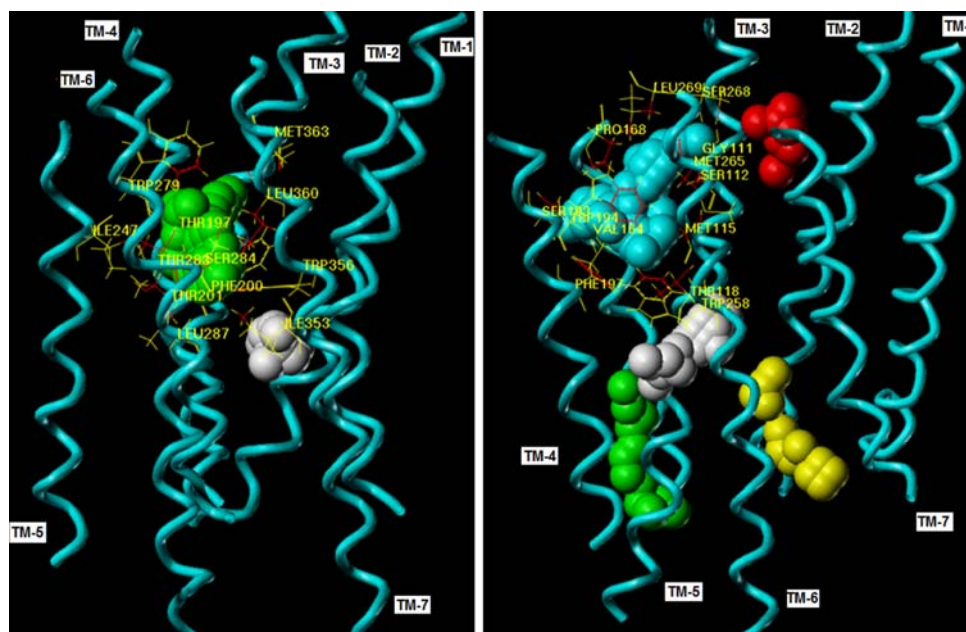


Fig. 4 Representative picture of AMG3 ligand in the lipid bilayer environment for the MD simulations

our group [35]. MD simulations of AMG3 in DMSO environment produced three more low energy conformers in addition to the previous ones. These conformers are called **a'**, **e'**, and **f'** and are shown in Fig. S1.

- (ii) *MD in DPPC bilayers*: Initial positions of the conformers in DPPC bilayers have been embedded according to experimental findings. Alkyl chain of conformers has been inserted through the alkyl chains of the lipid (parallel orientation with lipid chains), and rigid segment of the AMG3 was localized close to the head groups of DPPC and to orient their long axis perpendicular to the bilayer plane (Fig. 4). Results of MD simulations have shown that, optimal conformation is the *all*

Fig. 5 Proposed binding pockets for CB1 (left) and CB2 receptor models (right) by Biopolymer module of Sybyl



trans at dihedral angles τ_3 – τ_6 of alkyl chain for all of the presented conformers of AMG3, as it is observed in the MD simulations in DMSO environment. Torsional angles of alkyl side chain of conformer **a** did not change through simulations with small perturbations around initial value. Conformers **aa**, **b**, and **e** have been changed to conformer **f'** throughout the simulations. Conformer **c** has been transformed to conformers **b** and **a'**, while conformer **d** has been transformed to conformer **b**. Conformers **f** and **h** have been transformed to conformers **e**, **e'**, and **f'**. Conformer **g** has been transformed to conformers **b** and **a'**. The trajectory analyses of the torsional angles at the alkyl side chain of the conformers are shown in the Fig. S2 of the Supporting Material.

Both in DMSO and in DPPC bilayers, the MD simulations results produce same stable conformers **a**, **b**, **e**, **a'**, **e'**, and **f'**. These conformers have *gauche* \pm for τ_1 , *gauche* \pm and *trans* for τ_2 , and *all trans* conformations for τ_3 – τ_6 dihedral angles. These results validate the use of DMSO molecules as a source of amphiphilic environment, which mimics physiological conditions. The above mentioned stable favorable conformers in solution have been considered for further investigation.

Molecular docking studies

The 3D models of the CB1 and CB2 receptors were constructed by several groups [64–66] with a molecular modeling procedure, using the X-ray structure of bovine rhodopsin [67] as the initial template and taking into account the available site-directed mutagenesis data. The 3D models of CB receptors were borrowed from Tuccinardi et al.

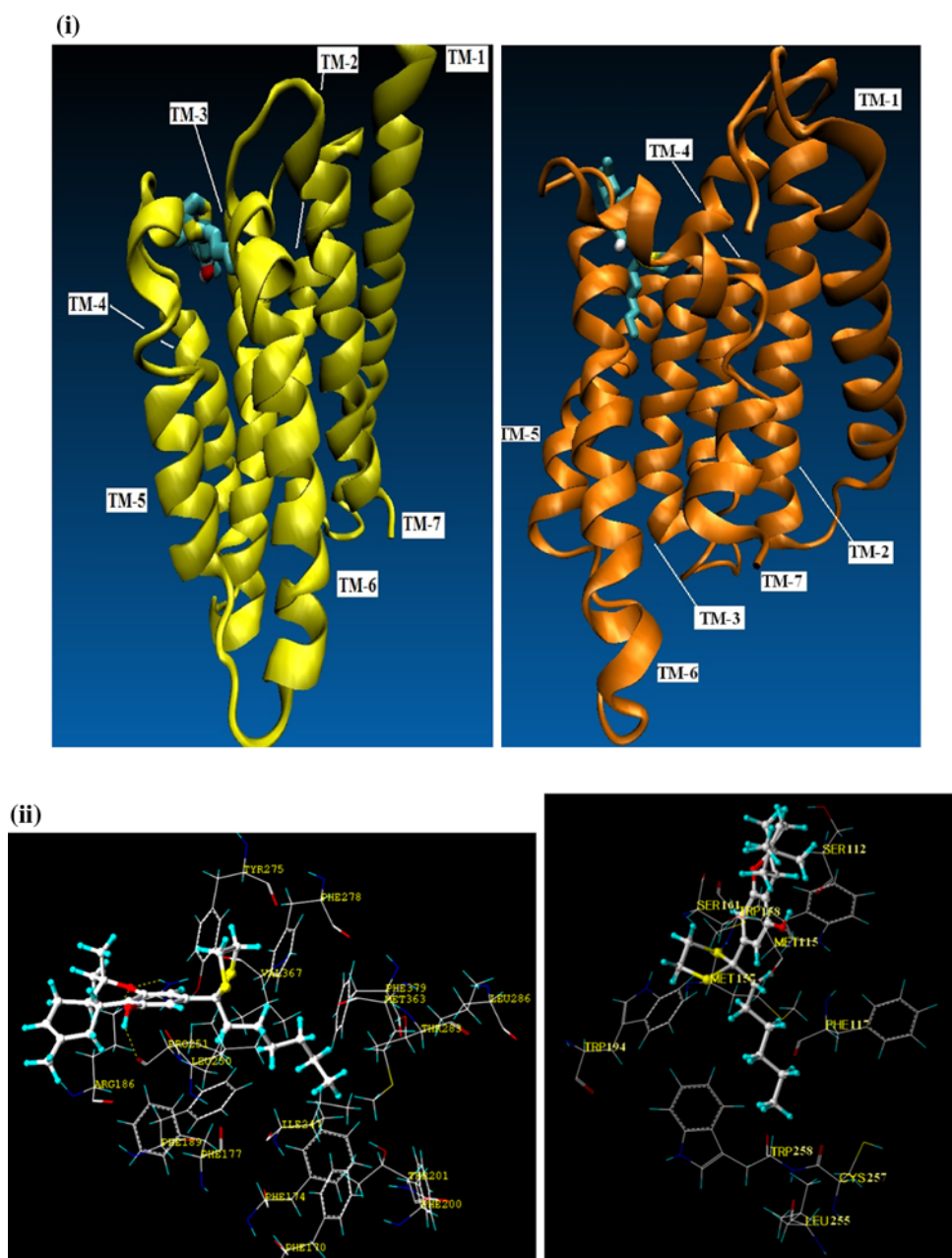
Table 3 The mean, the highest and the lowest values of the best thirty binding scores for each complex of the (i) CB1 and (ii) CB2 receptors and AMG3 conformers as well as the standard deviations between the binding scores are presented

Conformer	Mean ^a	Highest ^a	Lowest ^a	Std. Dev.
(i)				
a	−9.93	−11.40	−9.26	0.60
b	−10.15	−11.43	−9.50	0.56
e	−9.50	−10.86	−8.90	0.46
a'	−9.77	−11.14	−9.18	0.49
e'	−9.55	−10.67	−9.01	0.44
f'	−9.55	−11.15	−9.07	0.49
(ii)				
a	−9.82	−11.50	−9.31	0.48
b	−10.26	−12.52	−10.26	0.69
e	−8.38	−9.22	−8.15	0.25
a'	−10.29	−11.80	−9.73	0.55
e'	−9.35	−11.15	−9.35	0.66
f'	−8.90	−10.66	−8.26	0.66

^a The mean, the highest and the lowest total scores by FlexX (Flexible Docking)

[66] and used in the docking simulations; however, the critical amino acids for the CB binding are determined considering all the models mentioned above. Tuccinardi et al. [66] mentioned that rhodopsin in its crystallized form is in the inactive state. For this reason, for making it suitable as a target for drug docking studies, they have modified it on the basis of the “receptor activation” information. This TM helices of the modified models were readily provided to us for performing our described research activity. The ligand-binding pockets of the receptors have been obtained by the Biopolymer module of Sybyl molecular modeling package. Figure 5 shows the proposed binding pockets for the CB1 and CB2 receptors. Two binding pockets in the CB1 and five binding pockets in the CB2 receptors have

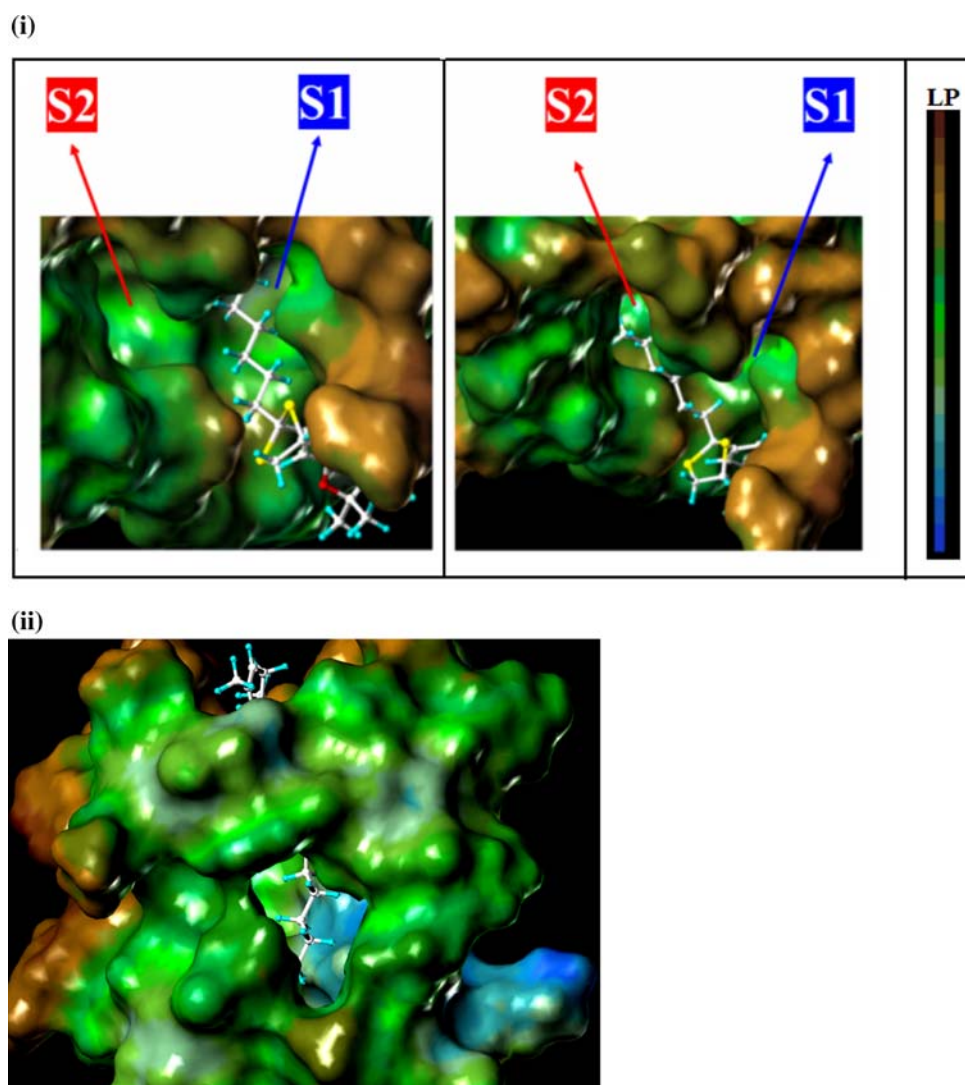
Fig. 6 (i) Ligand location at the active site of the receptors CB1 (*left*) and CB2 (*right*); (ii) AMG3 stabilizes its binding mainly through van der Waals interactions with the non-polar surfaces of the active site residues of CB1 receptor (*left*), (i.e., Lue193, Phe200, Thr201, Ile247, Pro251, Thr283, Trp356, Leu360, Val387) and CB2 receptor (*right*), (i.e., Phe117, Trp194, Leu255, Cys257, Trp258)



been determined. The largest cavities of the receptors found include same positions of the critical amino acids reported in the literature. Since conformers **a**, **b**, **e**, **a'**, **e'**, and **f'** are found the most favored stable conformers through MD simulations in solution, flexible docking has been employed to these six conformers using FlexX docking algorithm of Sybyl molecular modeling package [57]. FlexX is a docking method that uses an efficient incremental construction algorithm to optimize the interaction between a flexible ligand and a rigid binding site of the receptor. In this method, an empirically derived scoring function is used to predict the binding free energy. The active site in the docking runs included all atoms within a radius of 5.5 Å around the critical

amino acids for CB1: Phe174, Leu190, Lys192, Leu193, Gly195, Val196, Thr197, Phe200, Thr201, Pro251, Trp356, Leu359, Ser383, Cys386, Leu387 [64–66, 68–70], and for CB2: Leu108, Ser112, Pro168, Leu169, Trp194, Trp258 [66]. (The complete list of amino acid residues from the binding site is detailed in the Supporting Material.) The mean, the highest, and the lowest values of the best thirty binding scores for each complex of the CB1, CB2 receptors, and AMG3 conformers; as well as the standard deviations between the binding scores are presented in Table 3. Among the conformations, the conformer **b** of AMG3 is associated with the best binding energy with the active site residues for CB1 and CB2 receptors. Figure 6i shows the localization

Fig. 7 (i) The two cavities S1 and S2 observed at the active site of the CB1 receptor: S1 and S2 pockets constitute two cavities that have ~ 7 and ~ 10 Å depths, respectively, and they accommodate the alkyl chain segment of CBs. (ii) AMG3 ligand location at the CB2 receptor. MOLCAD lipophilic potential surface was calculated for the receptor with the Connolly method. *Brown color* denotes the most lipophilic areas and *blue color* denotes the most polar areas



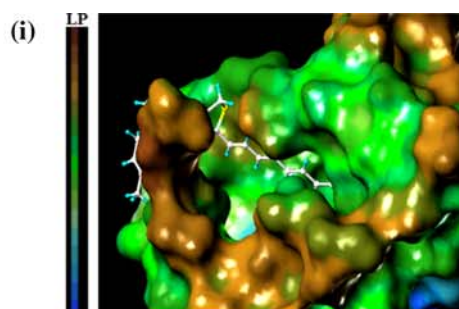
of AMG3 ligand at the binding sites of the CB1 (left) and CB2 (right) receptor models. Core of TM3–TM7 helices mainly participate to the binding cavities. Figure 6ii shows the interactions of binding site residues with the AMG3. The bioactive CB ligand AMG3 stabilizes its interactions with the active site through non-bonding van der Waals interactions with the non-polar surfaces of the active site residues of CB1 receptor (i.e., Leu193, Phe200, Thr201, Ile247, Pro251, Thr283, Trp356, Leu360, Val387) and CB2 receptor (i.e., Phe117, Leu194, Leu255, Trp258). The main characteristic of the low energy conformers of AMG3, both in solution and at the active site of the receptor, is the high flexibility of the alkyl side chain. This is eminent by the low energy barriers observed in the various low energy rotamers of the molecule. It is noticed that the CB1 receptor has two available pockets (namely S1 and S2) located at the binding site for the accommodation of CB ligands (Fig. 7i). S1 and S2 pockets constitute two cavities of ~ 7 Å and ~ 10 Å

depths, respectively. They both can accommodate the alkyl side chain segment of CB ligands. Our findings are in accordance with previous reports [22], which show that extension of the five carbon atom chain (~ 7 Å) of THC by one or two carbon atoms (~ 10 Å) improves binding, while further extension (> 10 Å) is detrimental due to steric hindrance. However, CB2 receptor has only one ligand-binding pocket (Fig. 7ii). Population analysis of docking modes for both CB1 and CB2 receptors showed that conformer **b** has higher propensity to bind at the active site of the CB1 and CB2 receptors.

Molecular specificity for the S1 and S2 pockets at CB1 receptor

Since AMG3 has conformational flexibility that can accommodate S1 and S2 pockets at CB1 receptor, it should be of

Fig. 8 (i) Unsaturation of alkyl chain leads the orientation of chain towards S2. For this reason, a structure was designed possessing four unsaturated bonds which were directed specifically to S2 cavity. (ii) Docking of rationally designed AMG3 analogues possessing double bonds at the alkyl side chain of the CB1 receptor. The degree of unsaturation is critical for the design of analogues to orient toward S1 or S2 cavity. (iii) Total FlexX binding scores versus number of double bonds at the side chain. The optimal number of double bonds at the alkyl side chain is four at S2 cavity. * The best score obtained from 30 docking solutions

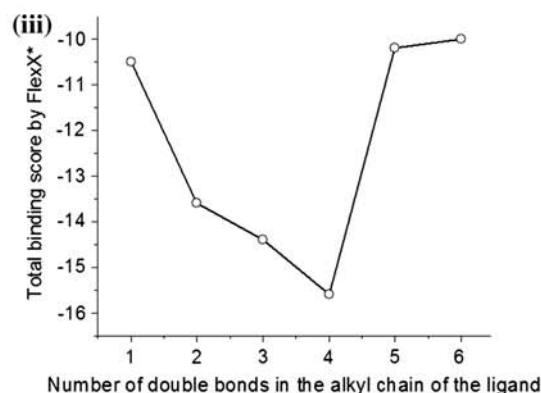
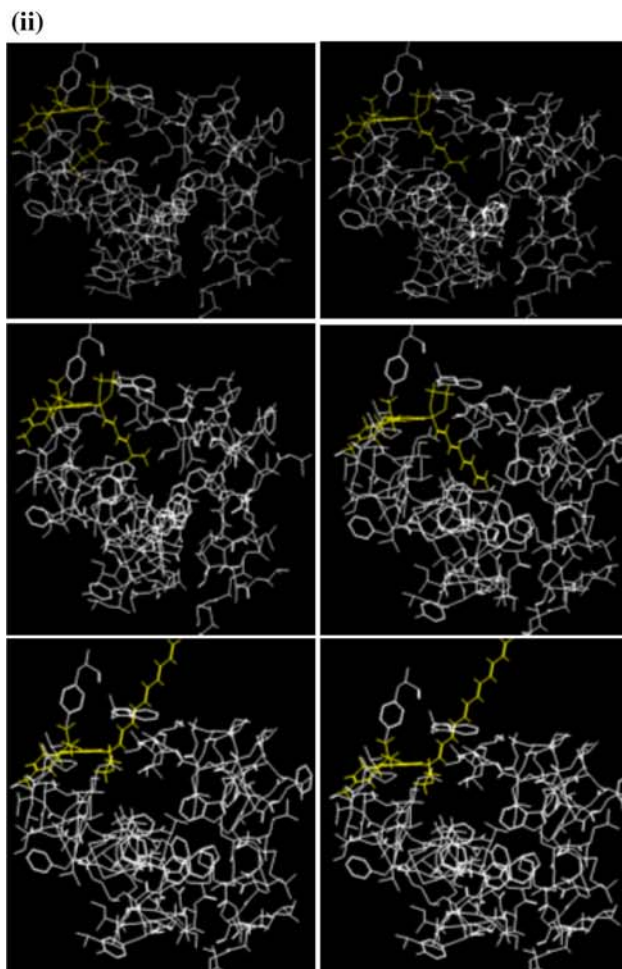


great interest to study the conformational preferences of these two cavities located at the binding site of the receptor. Design of molecules with specific preference to either site may be of high biological significance. S2 is deeper than S1 pocket and accommodates preferably the *all trans* conformation of the alkyl side chain segment of ligands. Unsaturation of the alkyl side chain of compounds leads their orientations toward S2 pocket. For this reason an analog of AMG3 with four unsaturated bonds at the alkyl chain was designed to specifically be directed to S2 cavity of the CB1 receptor (Fig. 8i).

These predictions have been tested with the docking trials of novel analogs possessing unsaturation of alkyl side chain of AMG3. Imposing double bond unsaturation to the C2'–C3' single bond of AMG3, is not enough for forcing the side chain toward lateral orientation (top-left on the Fig. 8ii). However, further unsaturation, namely, addition of double bonds to C4'–C5' (top-right on the Fig. 8ii) and C6'–C7' bonds (mid-left on the Fig. 8ii) leads the orientation of unsaturated alkyl chain toward S2 pocket. The four unsaturated bonded analog has optimum alkyl side chain length for the S2 pocket (mid-right on the Fig. 8ii). Further extension is detrimental (bottom on the Fig. 8ii). Figure 8iii depicts the total FlexX binding scores versus number of double bonds at the alkyl side chain segment of AMG3 analogs mentioned above. Different unsaturation patterns have been also studied at the alkyl side chain of AMG3 to cover all possible probabilities without accounting for the synthetic difficulty. For example, unsaturation of alkyl chain at the position of C2'–C3' and C5'–C6' has been performed. The docking results showed that, unsaturation leads to better binding scores than AMG3, however, it is not enough to orient to the direction of S2 site. The proposed molecules will be synthesized and tested for their biological activity to validate our rational design. Depending on the observed activity, we will be able to differentiate if optimum activity is induced by S1 or S2 pockets. These observations may help open new avenues to synthetic chemists for synthesizing novel compounds.

MD simulations of AMG3 at the active site of membrane-associated CB1 and CB2 receptors

MD simulations have been performed to the systems including AMG3 at the binding site of the CB1 and CB2 receptors



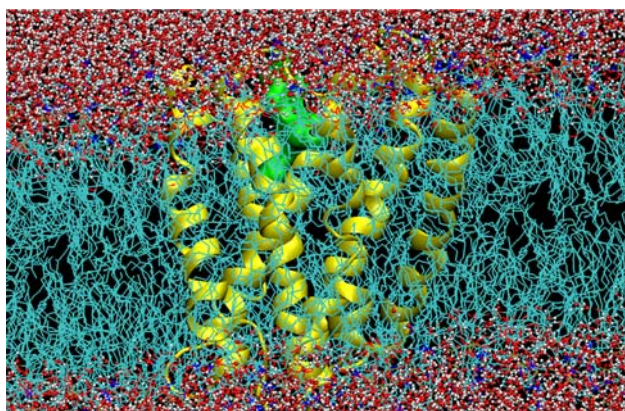


Fig. 9 Representative picture of used systems for MD simulations (a snapshot from MD simulations of AMG3 at the binding site of CB1 receptor merged with lipid bilayer)

merged with membrane bilayer to analyze the effect of critical amino acid residues at the active site of CB receptors to the conformational properties of ligand. Figure 9 shows a representative picture of used systems. For these simulations, docked poses of complexes that have high population were used as initial ligand-receptor complex coordinates. Torsional angle values of the alkyl side chain of AMG3 throughout the simulations were screened with trajectory analysis. Results showed that adopted conformations of AMG3 at CB1 and CB2 receptors have different conformational properties. Torsional angles at the alkyl chain of AMG3 adopt *trans* for τ_1 , τ_3 , τ_5 and τ_6 at the binding site of CB2 receptor with some fluctuations near this dihedral angle. Trajectory analysis of torsional angles τ_2 shows a propensity to be *gauche*– at the binding site of the CB2. Torsional angle τ_4 adopts *gauche*– and *trans* dihedral angles at the active site of the CB2 receptor (Fig. S3). Dihedral angle screening throughout the MD simulations results showed that τ_2 , τ_4 and τ_6 mainly form a *trans* conformations at the binding site of the CB1 receptor. Dihedral angles τ_3 and τ_5 are very flexible and adopt *gauche* \pm and *trans* conformations at the binding site of the CB1 receptor, however, *gauche*+/*trans* and *trans*/*gauche*– torsional angles are mainly observed for τ_3 and τ_5 , respectively (Fig. S3).

Therefore, five additional conformations (**m**, **ab**, **ac**, **ad**, and **ae**) have been derived from these simulations (Fig. S4). Torsional angle screening results of MD analysis showed that conformers **b**, **ab**, **ac**, and **ad** of AMG3 favor at the active site of the CB1, and conformers **m** and **ae** favor at the binding site of the CB2 receptor.

Although the CB1 and CB2 receptors exhibit a very high sequence homology which rises to 68% in the TM regions, there are certain behavioral differences of AMG3 conformers at the binding sites of receptors. One of the main differences between the MD simulations of ligand at the CB1 and CB2 receptors is the different behavior of the first dihedral angle τ_1 of the alkyl side chain of AMG3. In the CB1 receptor,

there is a high propensity of τ_1 to establish a *gauche*+ conformation; however, in the CB2 receptor, it prefers to have a *trans* conformation. It is well known that, different conformational rearrangements of third and sixth TMs of GPCR determine the activation of CBs. In CB2 receptor, alkyl side chain of AMG3 conformers align parallel in the ligand recognition part of TM3, while in the CB1 receptor they align perpendicular. This observation may help to understand the selectivity of CB ligands for the CB1 and CB2 receptors.

Homology modeling of CB1 and CB2 receptors based on β 2-adrenergic receptor

In order to validate the obtained results using CB1 and CB2 receptor models based on rhodopsin, alternative CB1 and CB2 comparative models have been performed employing template structure of β 2-adrenergic receptor. The initial structure was taken from the cholesterol bound form of human β 2 adrenergic receptor (PDB code: 3D4S) [37]. The water molecules and the cholesterol were removed from the system. Sequence alignment has been obtained with Biopolymer module of Sybyl. CB1 and CB2 receptors show 28% and 24% sequence identity, respectively (Supporting Material, Fig. S5). Initial geometry optimization calculations have been carried out with Powel algorithm using Tripos force field. Subsequently, these receptors have been subjected to 1 ns MD simulations. Before the simulations, geometry optimization of receptors have been performed without constraints using steepest descent integrator for 10,000 steps with the minimization tolerance of $100 \text{ kJ} (\text{mol nm})^{-1}$. Cluster analysis of obtained coordinate file of trajectories has been performed with *g_cluster* module of Gromacs and each simulation yielded 8 clusters. Sequence alignment of representative of these clusters with the rhodopsin based receptor models have been performed with Accelrys DS 2.0 program. Results showed that fourth member (Fig. S6, left) of the cluster at CB1 model and third member (Fig. S6, right) of the cluster at CB2 model have smaller total RMSD values (using C^α atoms as reference points) than other members. The number of conformers at each cluster and their total RMSD values has been given in Table 4. Obviously there are some fine differences between the two models for each receptor; however, the motifs of the seven member TM helices have been kept. It should be noted that the active site residues have smaller RMSD values than the other amino acid residues. For clarity, superimposition of rhodopsin and β 2-adrenergic based receptor models of CB1 has been shown at Fig. 10. In Fig. 11, the ligand-binding pockets have been shown with novel obtained model of CB1 receptor. The figure clearly confirms the two obtained binding pockets from the previous model. Three binding pockets (P1–P3) of CB1 receptor have been reported by Shim et al. [70]. The binding pockets presented in this work and Shim et al. [70] have similar binding

Table 4 Cluster analysis of obtained receptor models based on β 2-adrenergic receptor

Model number	Number of conformers in each model		RMSD (Å), CB1	RMSD (Å), CB2
	CB1	CB2		
1	309	258	6.74	5.50
2	260	243	6.91	5.39
3	180	149	6.86	5.08
4	128	143	6.62	5.47
5	64	95	6.72	5.40
6	34	45	6.63	5.58
7	13	37	6.78	5.24
8	12	30	6.72	5.52

The members of conformers at each family and their RMSD values between corresponding rhodopsin based homology models (reference points: C $^{\alpha}$ atoms)

site residues. However, depending on the model used, these cavities that accommodated the ligands may vary in the shape. Nevertheless, the binding pocket S2 is the common binding pocket found by Shim et al. [70] and designated as P2.

De novo drug design studies

In order to propose new analogs of AMG3, in addition to previously presented unsaturated analogs, a de novo drug design study using Leapfrog program under Sybyl molecular modeling package was performed based on derived conformations of AMG3 at the binding sites of the CB1 and CB2 membrane-associated receptors. Initial docking results showed that conformers **ad** and **ae** produced higher binding scores for CB1 and CB2 receptors, respectively. Therefore, de novo analysis is initiated using these conformers as well as

previously derived unsaturated analog of AMG3 that has the highest binding score. Tables 5 and 6 show proposed analogs for CB1 and CB2 receptors and their binding scores (only compounds that have better binding score than reference compounds were presented). Predicted high binding affinities of proposed compounds were confirmed by better docking scores than AMG3 (i.e., **D1** and **D10** have binding scores as -17.50 and -15.10 kJ mol $^{-1}$, respectively). In Fig. 12, binding interactions of proposed analogs of AMG3 that have the best binding scores for CB1 and CB2 receptors (**D1** and **D10**, respectively) were shown. The **D1** stabilizes its interactions with the binding site forming H-bonds with the amino acid residues (e.g., Arg186, Thr197, and Pro251) of CB1, as well as van der Waals interactions with the non-polar surfaces of the active site residues of CB1 receptor (e.g., Thr197, Phe200, Thr201, Ile247, Leu250, Pro251, Tyr275, Trp279, Thr283, Leu360). The **D10** stabilizes its interactions with the binding site forming H-bonds with the amino acid residues (e.g., Leu160, Leu163, Ser165, Tyr166, Leu167, Pro168) as well as van der Waals interactions with the non-polar surfaces of the binding site residues of CB2 receptor (e.g., Lys109, Leu160, Leu163, Pro168, Pro187, Tyr190, Trp194, Trp258).

Conclusions

In this study, we have applied a systematic approach to examine the putative bioactive conformations of flexible potent CB molecule AMG3 in solution and at the active site of the membrane-associated CB receptors. Our conformational analysis studies starts with classical methods, namely MC conformational search analysis and classification of produced

Fig. 10 Superimposition of rhodopsin (yellow colored)- and β 2-adrenergic (cyan colored)-based CB1 receptor models from both side and top views

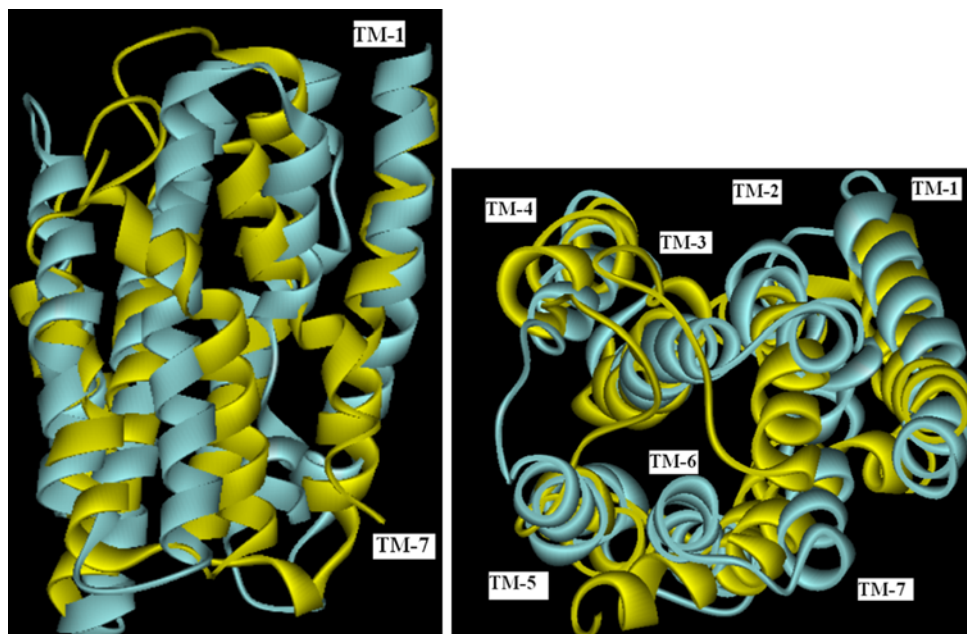


Fig. 11 CB1 receptor model obtained by using template of human β 2-adrenergic receptor (*right*) also showed two ligand-binding pockets between the TM3–TM6 as it is observed in the CB1 receptor model based on rhodopsin (*left*)

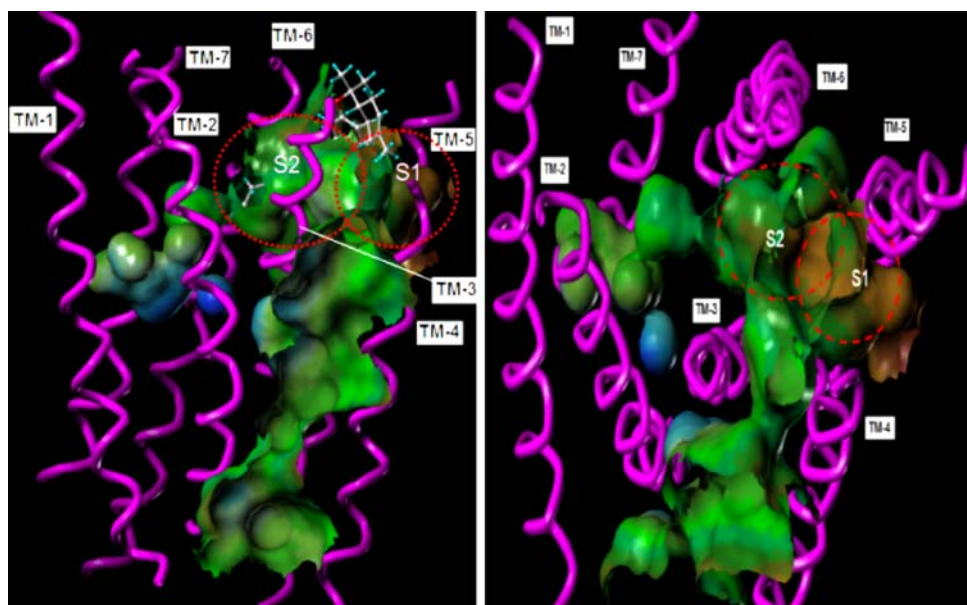


Table 5 Proposed analogues of AMG3 for CB1 receptor (only compounds that have better binding score than reference compounds are presented)

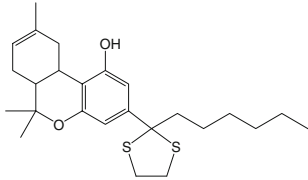
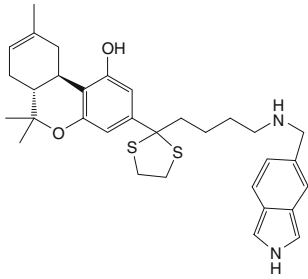
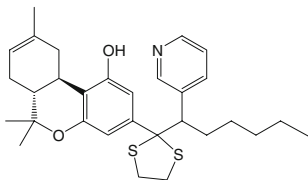
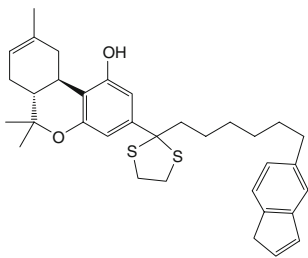
Compound	Docking score (kJ mol ⁻¹)
Ref. 1 (conf. ad of AMG3)	-12.50
	-12.50
D1	-17.50
	-17.50
D2	-17.01
	-17.01
D3	-16.94
	-16.94

Table 5 continued

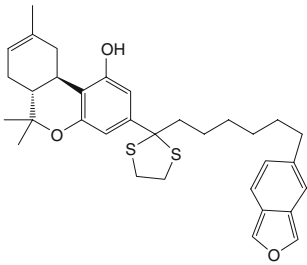
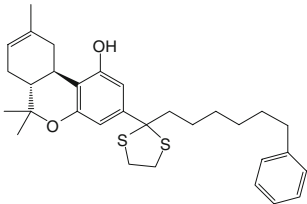
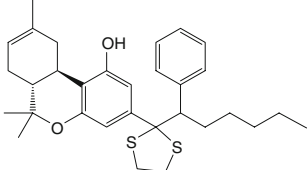
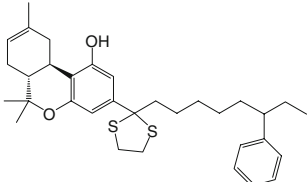
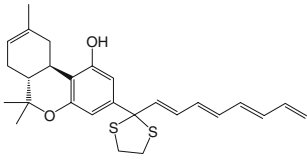
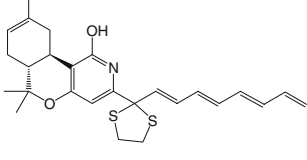
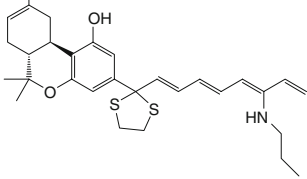
Compound		Docking score (kJ mol ⁻¹)
D4		-16.46
D5		-16.27
D6		-14.30
D7		-13.00
Ref. 2		-15.50
D8		-16.45
D9		-16.06

Table 6 Proposed analogues of AMG3 for CB2 receptor (only compounds that have better binding score than reference compound are presented)

Compound		Docking score (kJ mol ⁻¹)
Ref. (conf. ae of AMG3)		-12.70
D10		-15.10
D11		-13.27
D12		-12.93

conformers. The lowest energy conformer from each family has been picked up and was considered for further analysis. The MM/QM geometry optimization calculations were performed, both in vacuum and continuum DMSO environment. In addition, semi-empirical rotational energy barrier calculations have been studied for the flexible alkyl chain of ligand. The solvent and temperature effects on the conformers have been analyzed by using MD “in solution” simulations. Trajectory analysis results from flexible alkyl chain torsional angles give their favored adopting dihedral angle values in explicit DMSO solvent as well as DPPC lipid bilayer environments. These results allow a direct comparison with those obtained by MC. Subsequently, the stable conformers in solution have been selected from MD simulations and for these conformations of AMG3, *in silico* docking calculations have been performed at the rhodopsin based CB1 and CB2 receptor models. Docked poses of conformers at the active sites of both CB1 and CB2 receptors have been analyzed based on dihedral angle values of their alkyl chain. In order to examine the stability of conformers at the binding sites, MD simula-

tions have been performed in membrane-associated receptor models. Trajectory analysis from MD simulations has been reanalyzed to examine their favored adopting dihedral angle values at the binding sites of the receptors. The performed trajectory analysis of MD simulations results showed that wrapped conformations of alkyl chain in solution are dynamically less favorable than the *all trans* dihedral angles. The obtained different orientations at the active site of the CB1 and CB2 receptors from membrane-associated MD trajectory analysis can be used to synthesize more selective CB ligands. Bovine rhodopsin-based CB1 receptor model gave two different binding sites. Since properties of the obtained binding cavities depend on the used model, obtained results have to be rechecked using other receptor models. For this reason, homology modeling studies have been performed using β 2-adrenergic receptor models. The obtained models confirmed the derived ligand-binding pockets.

This study offers a stepwise conformational analysis, which leads to thorough and fruitful investigation of favored adopting conformers in solution and at the active site of the

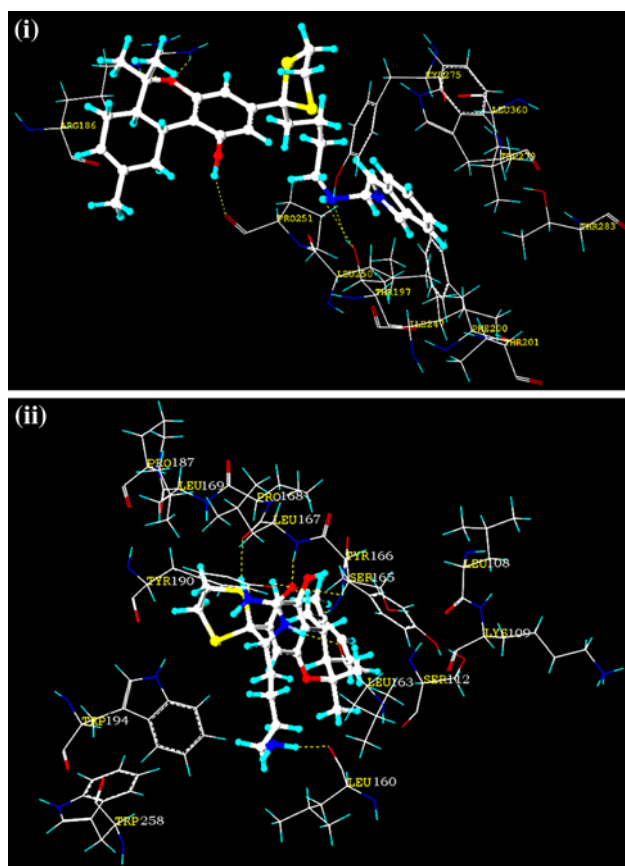


Fig. 12 (i) Binding interactions of **D1** at the binding site of the CB1 receptor; (ii) binding interactions of **D10** at the binding site of the CB2 receptor

membrane-associated receptors. The results of this study are not limited with the CB ligands but they can be extended to any amphotheric flexible molecule. Thus, the applied strategy may widen the scope of drug design.

Acknowledgments This study was financially supported by the European Union within sixth Framework Programme-Marie Curie Actions (Project: EURODES-MEST-CT-2005-020575). We thank Prof. A. Martinelli and his research group (Dipartimento di Scienze Farmaceutiche, Università di Pisa) for sharing their constructed TM helices of CB1 and CB2 receptors.

References

- Höltje HD, Sippl W, Rognan D, Folkers G (2003) Molecular modeling: basic principles and applications. 2. Wiley-VCH Verlag GmbH, Weinheim
- Ghose AK, Crippen GM, Revenkar GR, Smee DF, McKernan PA, Robins RK (1989) Analysis of the in vitro antiviral activity of certain ribonucleosides against parainfluenza virus using a novel computer aided receptor modeling procedure. *J Med Chem* 32:746–756
- Lenkinski RE, Stephens RL, Krishna NR (1981) Conformation of angiotensin II. Evidence for a specific hydrogen bonded conformation. *Biochemistry* 20:3122–3126

- Sakarellos C, Lintner K, Piriou F, Femandjian S (1983) Conformation of the central sequence of angiotensin II and analogs. *Bio-polymers* 22:663–687
- Femandjian S, Fromageot P, Tistchenko AM, Leicknam JP, Lutz M (1972) Angiotensin II conformations. Infrared and Raman studies. *Eur J Biochem* 28:174–182
- Mavromoustakos T, Theodoropoulou E, Zervou M, Kourouli T, Papahatjis DP (1999) Structure elucidation and conformational properties of synthetic cannabinoids (-)-2-(6a,7,10,10a-tetrahydro-6,6,9-trimethyl-1-hydroxy-6H-dibenzo[b,d]pyranyl)-2-hexyl-1,3-dithiolane and its methylated analog. *J Pharm Biomed Anal* 18:947–956
- Papahatjis DP, Nikas SP, Kourouli T, Chari R, Xu W, Pertwee RG, Makriyannis A (2003) Pharmacophoric requirements for the cannabinoid side chain. Probing the cannabinoid receptor subsite at C1'. *J Med Chem* 46:3221–3229
- Honorio KM, da Silva ABF (2002) A theoretical study on the influence of the frontier orbitals HOMO and LUMO and the size of C4 and C2 substituents in the psychoactivity of cannabinoid compounds. *Theochemistry* 578:111–117
- Keimowitz AR, Martin BR, Razdan RK, Mascarella SW, Thomas BF (2000) QSAR analysis of Δ^8 -THC analogues: relationship of side-chain conformation to cannabinoid receptor affinity and pharmacological potency. *J Med Chem* 43:59–70
- Schmetzer S, Greenidge P, Kovar KA, Schulze-Alexandru M, Folkers G (1997) Structure-activity relationships of cannabinoids: a joint CoMFA and pseudoreceptor modelling study. *J Comput Aided Mol Des* 11:278–292
- Najmanovich R, Kuttner J, Sobolev V, Edelman M (2000) Side-chain flexibility in proteins upon ligand binding. *Proteins Struct Funct Bioinf* 39:261–268
- Jorgensen WL (1991) Rusting of the lock and key model for protein-ligand binding. *Science* 254:954–963
- Hasegawa K, Arakawa M, Funatsu K (2003) Simultaneous determination of bioactive conformations and alignment rules by multi-way PLS modeling. *Compt Biol Chem* 27:211–216
- Papahatjis DP, Kourouli T, Abadji V, Goutopoulos A, Makriyannis A (1998) Pharmacophoric requirements for cannabinoid side chains: multiple bond and C1'-substituted Δ^8 -tetrahydrocannabinols. *J Med Chem* 41:1195–1200
- Razdan RK (1986) Structure-activity relationships in cannabinoids. *Pharmacol Rev* 38:75–149
- Makriyannis A, Rapaka RS (1990) The molecular basis of cannabinoid activity. *Life Sci* 47:2173–2184
- Durdagi S, Kapou A, Kourouli T, Andreou T, Nikas SP, Nahmias VR, Papahatjis DP, Papadopoulos MG, Mavromoustakos T (2007) The application of 3D-QSAR studies for novel cannabinoid ligands substituted at the C1' position of the alkyl side chain on the structural requirements for binding to cannabinoid receptors CB1 and CB2. *J Med Chem* 50:2875–2885
- Durdagi S, Papadopoulos MG, Papahatjis DP, Mavromoustakos T (2007) Combined 3D QSAR and molecular docking studies to reveal novel cannabinoid ligands with optimum binding activity. *Bioorg Med Chem Lett* 17:6754–6763
- Xie XQ, Pavlopoulos S, DiMeglio CM, Makriyannis A (1998) Conformational studies on a diastereoisomeric pair of tricyclic non-classical cannabinoids by NMR spectroscopy and computer molecular modeling. *J Med Chem* 41:167–174
- Xie XQ, Yang DP, Melvin LS, Makriyannis A (1994) Conformational analysis of the prototype nonclassical cannabinoid CP-47,497, using 2D NMR and computer molecular modeling. *J Med Chem* 37:1418–1426
- Xie XQ, Melvin LS, Makriyannis A (1996) The conformational properties of the highly selective cannabinoid receptor ligand CP-55,940. *J Biol Chem* 271:169–189

22. Reggio PH (2003) Pharmacophores for ligand recognition and activation/inactivation of the cannabinoid receptors. *Curr Pharm Des* 99:1607–1633
23. Song ZH, Slowey CA, Hurst DP, Reggio PH (1999) The difference between the CB1 and CB2 cannabinoid receptors at position 5.46. Is crucial for the selectivity of WIN55212-2 for CB2. *Mol Pharmacol* 56:834–840
24. Makriyannis A (1995) The role of cell membranes in cannabinoid activity. In: Pertwee R (ed) *Cannabinoid receptors*. Academic Press Limited, London, pp 87–115
25. Mavromoustakos T, Zervou M, Zoumpoulakis P, Kyrikou I, Benetis NP, Polevaya L, Roumelioti P, Giatas N, Zoga A, Moutevelis Minakakis P, Kolocouris A, Vlahakos D, Golic Grdadolnik S, Matsoukas J (2004) Conformation and bioactivity. Design and discovery of novel antihypertensive drugs. *Curr Top Med Chem* 4:385–401
26. Mavromoustakos T, Papahatjis D, Laggner P (2001) Differential membrane fluidization by active and inactive cannabinoid analogues. *Biochim Biophys Acta* 1512:183–190
27. Mavromoustakos T, Daliani I (1999) Effects of cannabinoids in membrane bilayers containing cholesterol. *Biochim Biophys Acta* 1420:252–265
28. Mavromoustakos T, Yang DP, Makriyannis A (1995) Small angle X-ray diffraction and differential scanning calorimetric studies on *O*-methyl-(-)- Δ^8 -tetrahydrocannabinol and its 5' iodinated derivative in membrane bilayers. *Biochim Biophys Acta* 1237:183–188
29. Yang DP, Mavromoustakos T, Beshah K, Makriyannis A (1992) Amphipathic interactions of cannabinoids with membranes. A comparison between Δ^8 -THC and its *O*-methyl analog using differential scanning calorimetry, X-ray diffraction and solid state deuterium NMR experiments. *Biochim Biophys Acta* 1103:25–36
30. Van der Schyf CJ, Mavromoustakos T, Makriyannis A (1988) The conformation of (-)- 8α and (-)- 8β -hydroxy- δ^9 -tetrahydrocannabinols and their interactions with model membranes. *Life Sci* 42:2231–2239
31. Mavromoustakos T, Yang DP, Broderick W, Fournier D, Herbette LG, Makriyannis A (1991) Small angle X-ray diffraction studies on the topography of cannabinoids in synaptic plasma membranes. *Pharmacol Biochem Behav* 40:547–552
32. Yang DP, Mavromoustakos T, Makriyannis A (1993) Small angle X-Ray diffraction studies of Δ^8 -tetrahydrocannabinol and its *O*-methyl analog in membranes. *Life Sci* 53:117–122
33. Martel P, Makriyannis A, Mavromoustakos T, Kelly K, Jeffrey KR (1993) Topography of tetrahydrocannabinol in model membranes using neutron diffraction. *Biochim Biophys Acta* 1151:51–58
34. Mavromoustakos T, Theodoropoulou E, Papahatjis D, Kourouli T, Yang DP, Trumbore M, Makriyannis A (1996) Studies on the thermotropic effects of cannabinoids on phosphatidylcholine bilayers using differential scanning calorimetry and small angle X-ray diffraction. *Biophys Acta* 1281:235–244
35. Durdagi S, Reis H, Papadopoulos MG, Mavromoustakos T (2008) Comparative molecular dynamics simulations of the potent synthetic classical cannabinoid ligand AMG3 in solution and at binding site of the CB1 and CB2 receptors. *Bioorg Med Chem* 16:7377–7387
36. Yuzlenko O, Kiec-Kononowicz K (2009) Molecular modeling of A1 and A2A adenosine receptors: comparison of rhodopsin and beta2-adrenergic-based homology models through the docking studies. *J Comput Chem* 30:14–32
37. Hanson MA, Cherezov V, Griffith MT, Roth CB, Stevens RC (2008) A specific cholesterol binding site is established by the 2.8 Å structure of the human β_2 -adrenergic receptor. *Structure* 16:897–905
38. Brooks BR, Bruccoleri RE, Olafson BD, States DJ, Swaminathan S, Karplus MM (1983) CHARMM: a program for macromolecular energy, minimization, and dynamics calculations. *J Comput Chem* 4:187–217
39. Leach AR (2001) *Molecular modeling: principles and applications*. 2. Pearson Educ. Ltd., England 465–467
40. Powell MJD (1977) Restart procedures for the conjugate gradient method. *Math Prog* 12:241–254
41. Gasteiger J, Marsili M (1980) Iterative partial equalization of orbital electronegativity—a rapid access to atomic charges. *Tetrahedron* 36:3219–3228
42. Frisch MJ, Trucks GW, Schlegel HB, Scuseria GE, Robb MA, Cheeseman JR, Zakrzewski VG, Montgomery JA, Stratmann RE Jr, Burant JC, Dapprich S, Millam JM, Daniels AD, Kudin KN, Strain MC, Farkas O, Tomasi J, Barone V, Cossi M, Cammi R, Mennucci B, Pomelli C, Adamo C, Clifford S, Ochterski J, Petersson GA, Ayala PY, Cui Q, Morokuma K, Malick, DK, Rabuck AD, Raghavachari K, Foresman JB, Cioslowski J, Ortiz JV, Baboul AG, Stefanov BB, Liu G, Liashenko A, Piskorz P, Komaromi I, Gomperts R, Martin RL, Fox DJ, Keith T, Al-Laham MA, Peng CY, Nanayakkara A, Gonzalez C, Challacombe M, Gill PMW, Johnson BG, Chen W, Wong MW, Andres JL, Head-Gordon M, Replogle ES, Pople JA (1998) Gaussian 98 revision A.9. Gaussian Inc., Pittsburgh
43. Schuettelkopf AW, van Aalten DMF (2004) PRODRG: a tool for high-throughput crystallography of protein-ligand complexes. *Acta Cryst D* 60:1355–1363
44. Lindhal E, Hess B, van der Spoel D (2001) GROMACS 3.0: a package for molecular simulation and trajectory analysis. *J Mol Model* 7:306–317
45. Berendsen HJC, Postma JPM, van Gunsteren WF, Dinola A, Haak JR (1984) Molecular dynamics with coupling to an external bath. *J Chem Phys* 81:3684–3690
46. Essmann U, Perera L, Berkowitz ML, Darden T, Lee H, Pedersen LG (1995) A smooth particle mesh Ewald method. *J Chem Phys* 103:8577–8592
47. Hess B, Bekker H, Berendsen HJC, Fraaije JGEM (1997) LINCS: a linear constraint solver for molecular simulations. *J Comput Chem* 18:1463–1472
48. Humphrey W, Dalke A, Schulten K (1996) VMD: visual molecular dynamics. *J Mol Graph* 14:33–38
49. Originlab Corporation, Northampton, MA 01060, USA. <http://www.originlab.com>
50. Patra M, Karttunen M, Hyvönen M, Falck E, Vattulainen P (2004) Lipid bilayers driven to a wrong lane in molecular dynamics simulations by subtle changes in long-range electrostatic interactions. *J Phys Chem B* 108:4485–4494
51. Patra M, Karttunen M, Hyvonen M, Falck E, Lindqvist P, Vattulainen I (2003) Molecular dynamics simulations of lipid bilayers: major artifacts due to truncating electrostatic interactions. *Biophys J* 84:3636–3645
52. van Gunsteren WF, Billeter SR, Eising AA, Hunenberger PH, Kruger P, Mark AE, Scott WRP, Tironi IG (1996) *Biomolecular simulation: the GROMOS96 manual and user guide*. Vdf Hochschulverlag AG an der ETH, Zurich
53. Parrinello M, Rahman A (1981) Polymorphic transitions in single crystals: a new molecular dynamics method. *J Appl Phys* 52:7182–7190
54. Kandt C, Ash WL, Tieleman DP (2007) Setting up and running molecular dynamics simulations of membrane proteins. *Methods* 41:475–488

55. Li J, Edwards PC, Burghammer M, Villa C, Schertler GF (2004) Structure of bovine rhodopsin in a trigonal crystal form. *J Mol Biol* 343:1409–1438
56. Böhm HJJ (1994) On the use of LUDI to search the fine chemicals directory for ligands of proteins of known three-dimensional structure. *Comput Aided Mol Des* 10:427–440
57. SYBYL v. 6.8. (2001) Molecular modeling software package. Tripos Inc., St. Louis
58. Becke AD (1993) Density functional thermochemistry. III. The role of exact exchange. *J Chem Phys* 98:5648–5662
59. Hehre WJ, Ditchfield R, Pople JA (1975) Self-consistent molecular orbital methods. XV. Extended Gaussian-type basis sets for lithium, beryllium, and boron. *J Chem Phys* 62:2921–2923
60. Soteriadou K, Tzinia AK, Panou-Pamonis E, Tsikaris V, Sakarellos-Daitsiotis M, Sakarellos C, Papapoulou Y, Matsas R (1996) Antigenicity and conformational analysis of the Zn²⁺ binding sites of two Zn²⁺ metalloproteases: Leishmania gp63 and mammalian endopeptidase-24.11. *Biochem J* 313:455–466
61. Stewart JJP (1989) Optimization of parameters for semiempirical methods I. Method. *J Comput Chem* 10:209–220
62. Durdagi S, Hofer TS, Randolph BR, Rode BM (2005) Structural and dynamical properties of Bi³⁺ in water. *Chem Phys Lett* 406:20–23
63. van Der Spoel D, Lindahl E, Hess B, Groenhof G, Mark AE, Berendsen HJ (2005) GROMACS: fast, flexible, and free. *J Comput Chem* 26:1701–1718
64. Salo OMH, Lahtela-Kakkonen M, Gynther J, Jarvinen T, Poso A (2004) Development of a 3D model for the human cannabinoid CB1 receptor. *J Med Chem* 47:3048–3057
65. Shim JY, Welsh WJ, Howlett AC (2003) Homology model of the CB1 cannabinoid receptor: sites critical for nonclassical cannabinoid agonist interaction. *Biopolymers (Pept Sci)* 71:169–189
66. Tuccinardi T, Ferrarini PL, Manera C, Ortore G, Saccomanni G, Martinelli A (2006) Cannabinoid CB2/CB1 selectivity. Receptor modeling and automated docking analysis. *J Med Chem* 49: 984–994
67. Palczewski K, Kumasaka T, Hori T, Behnke CA, Motoshima H, Fox BA, Le Trong I, Teller DC, Okada T, Stenkamp RE, Yamamoto M, Miyano M (2000) Crystal structure of rhodopsin: a G protein-coupled receptor. *Science* 289:739–745
68. Tao Q, McAllister SD, Andreassi J, Nowell KW, Cabral GA, Hurst DP, Bachtel K, Ekman MC, Reggio PH, Abood ME (1999) Role of a conserved lysine residue in the peripheral cannabinoid receptor (CB2): evidence for subtype specificity. *Mol Pharmacol* 55: 605–613
69. Mahmoudian M (1997) The cannabinoid receptor: computer-aided molecular modeling and docking of ligand. *J Mol Graph Model* 15:149–153
70. Shim JY, Howlett AC (2006) WIN55212-2 Docking to the CB1 cannabinoid receptor and multiple pathways for conformational induction. *J Chem Inf Model* 46:1286–1300